Dynamic Response of Reinforced Concrete Structures to Seismic Events in Brazil

José Vittor S. Cóco and Mauro Schulz

Department of Civil Engineering,
Federal Fluminense University,
Av. Passo da Pátria, 156, Niterói, RJ 24210-240, Brazil

Summary

This paper presents a nonlinear seismic analysis methodology for reinforced concrete structures, applied to a typical Brazilian example. Rigorous seismic analysis is essential for critical structures, such as nuclear power plants, and in regions of Brazil susceptible to seismic activity. The methodology uses time-domain analysis with a 3D Timoshenko beam element to capture nonlinear behavior of concrete and steel. Nodal forces are obtained from earthquake accelerograms. The damping matrix is evaluated at each time step, with an implicit time integration algorithm ensuring equilibrium. Implemented in C++, the method is used to analyze a reinforced concrete building under a Brazilian earthquake with artificial ground motion. Safety guidelines follow Brazilian standards. Results confirm the method's effectiveness in assessing displacements, with high convergence supporting its numerical reliability for seismic analysis.

1 INTRODUCTION

Nonlinear dynamic analysis is significant in Brazil, particularly for structures in regions like Acre and southwestern Amazonas, as well as critical facilities such as nuclear power plants, where rigorous evaluation is necessary. One common approach in dynamic analysis is the Response Spectrum Method (RSM), which estimates dynamic responses by summing modal absolute values using techniques like the Square Root of the Sum of Squares and Complete Quadratic Combination. However, these methods may estimate only the absolute maximum normal forces and bending moments, without differentiating between compressive and tensile stresses—an important consideration for RC members. Therefore, a time-domain analysis is more appropriate for the design of RC structures.

This study presents a time-domain methodology for the seismic nonlinear analysis of a RC structure using a 3D frame finite element model based on Timoshenko beam theory. Material nonlinearity is considered for normal stresses, while linear approximations are assumed for shear stresses. Constitutive material relations from the literature ensure reliable stress-strain analysis. Equivalent nodal forces are derived from accelerograms. Newmark's implicit method and an iterative method are employed in the time integration process. This methodology is implemented in C++ and applied to an example of a building in Acre, Brazil, submitted to a typical Brazilian earthquake. The guidelines of [1] are followed.

2 FINITE ELEMENT FORMULATION

A four-node 3D beam finite element with rectangular cross-section is used in this research. Its formulation is based on Timoshenko's beam theory, as outlined in [2] for nonlinear systems. Geometric nonlinearity effects are neglected in this study.

Considering the hypothesis that plane sections remain plane but not necessarily perpendicular to the normal axis of the deformed beam, normal strain $\varepsilon_{11}(X_1)$ can be written in terms of the nodal normal strain component vector $\boldsymbol{\varepsilon}_n(X_1)$, i.e. $\varepsilon_{11}(X_1)=\mathbf{x}^T\boldsymbol{\varepsilon}_n(X_1)$, where the position vector is $\mathbf{x}=\begin{bmatrix}1 & X_2 & X_3\end{bmatrix}^T$, and X_i, $i=1,2,3$, are the local coordinates. Vector $\boldsymbol{\varepsilon}_n(X_1)$ is given by $\boldsymbol{\varepsilon}_n(X_1)=\mathbf{B}_n^T(X_1)\mathbf{u}$. $\mathbf{B}_n$ is the Lagragian interpolation matrix associated with normal strains, and $\mathbf{u}$ is the nodal displacement vector. Similarly, nodal shear strain component vector $\boldsymbol{\varepsilon}_s(X_1)$ is interpolated as $\boldsymbol{\varepsilon}_s(X_1) = \mathbf{B}_s^T(X_1)\mathbf{u}$, where $\mathbf{B}_n$ is the shear interpolation matrix.

The normal internal force vector $\mathbf{s}_n(X_1) = [N_1 \quad M_2 \quad M_3]^T = \int_A [1 \quad X_2 \quad X_3]^T \sigma_{11}\, dA$ is computed considering the nonlinear behavior of both steel and concrete and is determined through a numerical integration process. The normal stress σ_{11} is evaluated at the geometric center of the infinitesimal cross-sectional area dA. The nonlinear nature of $\mathbf{s}_n$ yields the following linear incremental relation:

$$\Delta\mathbf{s}_n = \mathbf{D}_n \Delta\boldsymbol{\varepsilon}_n = \mathbf{D}_n \mathbf{B}_n^T \Delta\mathbf{u} \quad ; \quad \mathbf{D}_n = \int_A \mathbf{x}\, E\, \mathbf{x}^T dA \tag{1}$$

where E is the tangent modulus of the constitutive stress-strain relation. In this study, shear strains and stresses are assumed to behave linearly, considering only the contribution of concrete. The shear internal force vector $\mathbf{s}_s(X_1) = [V_2 \quad V_3 \quad T_1]^T$ and its associated incremental equation are evaluated as

$$\mathbf{s}_s = \mathbf{D}_s \boldsymbol{\varepsilon}_s = \mathbf{D}_s \mathbf{B}_s^T \mathbf{u} \quad ; \quad \Delta\mathbf{s}_s = \mathbf{D}_s \Delta\boldsymbol{\varepsilon}_s = \mathbf{D}_s \mathbf{B}_s^T \Delta\mathbf{u} \tag{2}$$

where $\mathbf{D}_s$ is a diagonal 3×3 matrix, and its elements are $D_{s11} = D_{s22} = k_s GA$ and $D_{s33} = GJ$. The shear coefficient k_s is defined by [3]. G, A and J are the shear modulus, the cross-sectional area and the torsional stiffness, respectively.

The principle of minimum strain-energy yields the following equilibrium equation, as well as its associated linear incremental equation:

$$\mathbf{f} = \int_L \mathbf{B}_n \mathbf{s}_n\, dX_1 + \int_L \mathbf{B}_s \mathbf{s}_s\, dX_1 \quad ; \quad \Delta\mathbf{f} = \int_L \mathbf{B}_n \Delta\mathbf{s}_n\, dX_1 + \int_L \mathbf{B}_s \Delta\mathbf{s}_s\, dX_1 \tag{3}$$

where $\mathbf{f}$ is the restoring force vector, and L is the beam length. The substitution of equations (1) and (2) in the linear incremental relation from equation (3) yields the tangent stiffness matrix $\mathbf{K}$ as

$$\mathbf{K}\,\Delta\mathbf{u} = \Delta\mathbf{f} \quad ; \quad \mathbf{K} = \int_L \left(\mathbf{B}_n \mathbf{D}_n \mathbf{B}_n{}^T + \mathbf{B}_s \mathbf{D}_s \mathbf{B}_s{}^T\right) dX_1 \tag{4}$$

$\mathbf{K}$ and $\mathbf{f}$ are evaluated applying a reduced Gauss-Legendre quadrature rule.

3 CONCRETE STRESS-STRAIN MODEL

In this study, the concrete stress-strain constitutive relation follows the model proposed by [4], as modified by [5]. This model considers the behavior of concrete under loading-unloading cycles. Different monotonic curves are used for unconfined and confined concrete (Fig. 1 (right)). Hence, cross-sectional discretization must adequately account for unconfined and confined concrete zones, which are bounded by the stirrup-tie's outer face (Fig. 1 (left)).

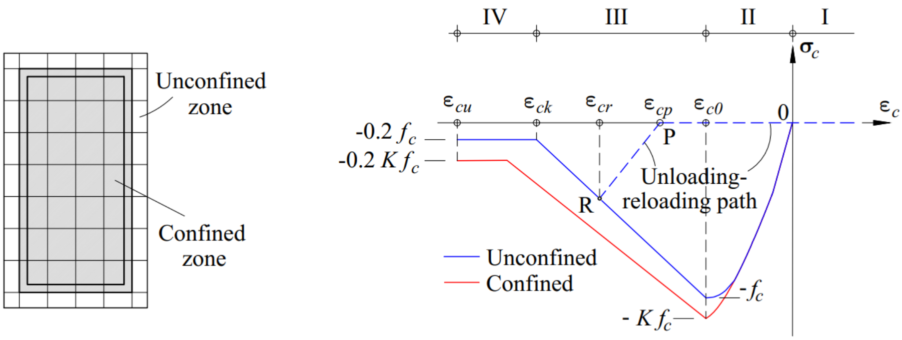

Fig. 1 Cross-sectional discretization in unconfined and confined concrete fibers (left). Concrete stress-strain model by [4] and [5] (right).

The trajectory of the monotonic curve in regions I, II, III and IV (Fig. 1 (right)) is given by

$$\sigma_c = \begin{cases} 0 & \text{for} \quad \varepsilon_c \geq 0 \quad (\text{Region I}) \\ -Kf_c\left[2\left(\dfrac{\varepsilon_c}{\varepsilon_{c0}}\right)-\left(\dfrac{\varepsilon_c}{\varepsilon_{c0}}\right)^2\right] & \text{for} \quad \varepsilon_{c0} \leq \varepsilon_c \leq 0 \quad (\text{Region II}) \\ \sigma_c = -K\, f_c\left[1 - Z\left(\varepsilon_{c0}-\varepsilon_c\right)\right] & \text{for} \quad \varepsilon_{ck} \leq \varepsilon_c \leq \varepsilon_{c0} \quad (\text{Region III}) \\ -0.2Kf_c & \text{for} \quad \varepsilon_{cu} \leq \varepsilon_c \leq \varepsilon_{ck} \quad (\text{Region IV}) \end{cases} \tag{5}$$

The concrete stress and strain are denoted by σ_c and ε_c, respectively. Factor K denotes the strength increase due to confinement and is defined as $K=1$, for unconfined concrete, and as $K = 1+\rho_s f_{yh}/f_c$, for confined concrete, where ρ_s is the ratio of the hoop set and concrete core volumes, f_{yh} is the yield strength of stirrups, and f_c is the concrete compressive strength. Tension stiffness is neglected in this model (region I). Region II is defined by the Hognestad parabola, in which $\varepsilon_{c0} = -0.002K$ is the strain at maximum compressive stress. Z is the slope of the post-yield line segment (region III) and is obtained according to the concrete confinement conditions. Strains ε_{ck} and ε_{cu} define the intersection between regions III and IV, and the ultimate strain, respectively. The latter is adopted as $\varepsilon_{cu} = -0.004$ and $\varepsilon_{cu} = -0.004 - 0.9\rho_s\left(f_{yh}/300\,\text{MPa}\right)$, for unconfined and confined concrete.

In the event of unloading, a reversal curve is started and follows a line segment that goes from reversal point R to a plastic point P at the σ_c axis (Fig. 1 (right)). Strain ε_{cr} is the reversal strain at R, while ε_{cp} is the plastic strain at P and is given by the following equation by [6]:

$$\varepsilon_{cp}/\varepsilon_{c0} = \begin{cases} 0.145\left(\varepsilon_{cr}/\varepsilon_{c0}\right)^2 + 0.127\left(\varepsilon_{cr}/\varepsilon_{c0}\right) & \text{for} \quad \varepsilon_{cr}/\varepsilon_{c0} < 2 \\ 0.707\left(\varepsilon_{cr}/\varepsilon_{c0} - 2\right) + 0.834 & \text{for} \quad \varepsilon_{cr}/\varepsilon_{c0} \geq 2 \end{cases} \tag{6}$$

The reversal trajectory follows $\sigma_c = 0$ for $\varepsilon_c \geq \varepsilon_{cp}$. If the trajectory returns to the original monotonic curve, new reversal curves may be their respective line segments RP, as defined by equation (6).

4 STEEL STRESS-STRAIN MODEL

This study follows the steel stress-strain model by [7]. This model accurately predicts the behavior of steel under cyclic loads, while simplifications proposed by [8] allow for proper computational implementation. The envelope monotonic curve is given by

$$\sigma_s = \begin{cases} -\sigma_{sy} + E_{s1}\left(\varepsilon_s - \varepsilon_{sy}\right) & \text{for} \quad \varepsilon_s \leq -\varepsilon_{sy} \\ E_{s0}\,\varepsilon_s & \text{for} \quad -\varepsilon_{sy} \leq \varepsilon_s \leq \varepsilon_{sy} \\ \sigma_{sy} + E_{s1}\left(\varepsilon_s - \varepsilon_{sy}\right) & \text{for} \quad \varepsilon_s \geq \varepsilon_{sy} \end{cases} \tag{7}$$

where the steel stress and strain are denoted by σ_s and ε_s, respectively. The steel stress and strain at yielding are $\sigma_{sy} = f_y$ and ε_{sy}, such that f_y is the steel tensile strength. Material parameter b is the ratio between the initial tangent modulus E_{s0} and the plastic slope E_{s1}, i.e. $E_{s1} = b\,E_{s0}$.

Reversal curves are started once unloading occurs at one of the post-yield line segments from equation (7), which are defined, in term of the normalized stress σ_s^* and strain ε_s^*, by

$$\sigma_s^* = b\varepsilon_s^* + (1-b)\varepsilon_s^* \Big/ \left(\left(1+\varepsilon_s^{*R}\right)^{1/R}\right) \quad ; \quad \sigma_s^* = \left(\sigma_s - \sigma_{sr}\right)/\left(\sigma_{s0} - \sigma_{sr}\right) \quad ; \quad \varepsilon_s^* = \left(\varepsilon_s - \varepsilon_{sr}\right)/\left(\varepsilon_{s0} - \varepsilon_{sr}\right) \tag{8}$$

where reversal point $\left(\varepsilon_{sr}, \sigma_{sr}\right)$ represents the start of reversal curve, and intersection point $\left(\varepsilon_{sr}, \sigma_{sr}\right)$ lies at the intersection between tangent lines l_e and l_p (Fig. 2 (left)). Parameter R defines the curvature of the reversal curve, considering the Bauschinger effect. This parameter is established according to ξ, which is obtained in relation to the maximum or minimum strain in history for upper or lower reversal curves, respectively, as suggested by [8] (Fig. 2 (right)).

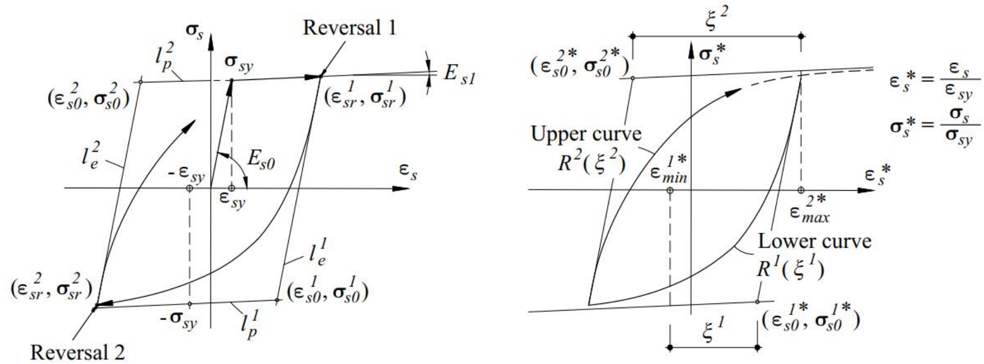

Fig. 2 Steel stress-strain reversal curves by [7] (left). Definition of parameter R by [8] (right).

On reversal curves, the tangent modulus of the steel stress-strain relation $\partial\sigma_s/\partial\varepsilon_s = \left(\partial\sigma_s/\partial\varepsilon_s^*\right)\left(\partial\varepsilon_s^*/\partial\varepsilon_s\right)$ is obtained according to equation (8). In order to avoid numerical issues due to discontinuity of derivatives at the start of a reversal curve, a linear approximation of $\partial\sigma_s/\partial\varepsilon_s$ is considered.

5 NEWMARK'S TIME INTEGRATION METHOD

The equation of motion of a nonlinear system is

$$\mathbf{M}\ddot{\mathbf{u}}(t) + \mathbf{C}\dot{\mathbf{u}}(t) + \mathbf{f}\left(\mathbf{u}(t)\right) = \mathbf{p}(t) \tag{9}$$

Nodal displacements $\mathbf{u}(t)$, nodal velocities $\dot{\mathbf{u}}(t) = d\mathbf{u}/dt$, nodal accelerations $\ddot{\mathbf{u}}(t) = d^2\mathbf{u}/dt^2$, and nodal external forces $\mathbf{p}(t)$ are defined at each time step $t = t_1, t_2, \ldots, t_i, t_{i+1}, \ldots, t_n$, where n is the number of time steps in which data from an accelerogram is analyzed. $\mathbf{M}$ is the mass matrix, which is simplified as a diagonal matrix in this work. $\mathbf{C}$ is the damping matrix, evaluated as a Rayleigh classic damping matrix, i.e.

$$\mathbf{C} = c_1\mathbf{M} + c_2\mathbf{K} \tag{10}$$

where parameters c_1 and c_2 are established according to the modal analysis of the associated undamped system, and tangent stiffness matrix $\mathbf{K}$ is established by equation (4). Restoring force vector $\mathbf{f}$ is obtained from equation (3). An analytical model to determine $\mathbf{p}$ after earthquake data from accelerograms is discussed in section 6 of this paper.

At time step $i+1$, $\dot{\mathbf{u}}(t_{i+1}) = \dot{\mathbf{u}}_{i+1}$ and $\ddot{\mathbf{u}}(t_{i+1}) = \ddot{\mathbf{u}}_{i+1}$ are implicitly approximated by Newmark's time integration method as

$$\dot{\mathbf{u}}_{i+1}(\mathbf{u}_{i+1}) = \frac{\gamma}{(\Delta t)\beta}(\mathbf{u}_{i+1} - \mathbf{u}_i) + \left(1 - \frac{\gamma}{\beta}\right)\dot{\mathbf{u}}_i + (\Delta t)\left(1 - \frac{\gamma}{2\beta}\right)\ddot{\mathbf{u}}_i \tag{11}$$

$$\ddot{\mathbf{u}}_{i+1}(\mathbf{u}_{i+1}) = \frac{1}{(\Delta t)^2\beta}(\mathbf{u}_{i+1} - \mathbf{u}_i) - \frac{1}{(\Delta t)\beta}\dot{\mathbf{u}}_i - \left(\frac{1}{2\beta} - 1\right)\ddot{\mathbf{u}}_i \tag{12}$$

Integration constants $\gamma = 1/2$ and $\beta = 1/4$ establish a linear and constant average approximations for equations (11) and (12), respectively, and guarantee numerical stability, according to [9]. Time interval $\Delta t = t_{i+1} - t_i$ should be small enough ($\Delta t > 0.02s$) to assure accurate response.

Displacement $\mathbf{u}(t_{i+1}) = \mathbf{u}_{i+1}$ ensures equilibrium if

$$\mathbf{g}(\mathbf{u}_{i+1}) = \mathbf{M}\ddot{\mathbf{u}}_{i+1} + \mathbf{C}\dot{\mathbf{u}}_{i+1} + \mathbf{f}(\mathbf{u}_{i+1}) - \mathbf{p}_{i+1} = \mathbf{0} \tag{13}$$

where $\mathbf{g}(\mathbf{u}_{i+1})$ is the residual function from equation (9) at time step $i+1$. Newton-Raphson iteration is performed to determine $\mathbf{u}_{i+1}$. At iteration $j+1$, $\mathbf{u}_{i+1}^{\langle j+1\rangle}$ is estimated as

$$\mathbf{u}_{i+1}^{\langle j+1\rangle} = \mathbf{u}_{i+1}^{\langle j\rangle} + \Delta\mathbf{u}_{i+1} \quad ; \quad \mathbf{K}_{eff}\,\Delta\mathbf{u}_{i+1} = -\mathbf{g}\left(\mathbf{u}_{i+1}^{\langle j\rangle}\right) \quad ; \quad \mathbf{K}_{eff} = \mathbf{M}\frac{1}{(\Delta t)^2\beta} + \mathbf{C}\left(\mathbf{u}_{i+1}^{\langle j\rangle}\right)\frac{\gamma}{(\Delta t)\beta} + \mathbf{K}\left(\mathbf{u}_{i+1}^{\langle j\rangle}\right) \tag{14}$$

At initial iteration $j = 0$, it is assumed $\mathbf{u}_{i+1}^{\langle 0\rangle} = \mathbf{u}_i$. Equation (14) is revaluated until the convergence criteria $\left\|\mathbf{g}(\mathbf{u}_{i+1})\right\| \le \text{tol}$ is satisfied, where $tol = 1\times10^{-4}$.

As stresses and strains are modified throughout the iterative process, the nonlinear stiffness matrix $\mathbf{K}$ is updated at every iteration. The nonlinearity of damping matrix $\mathbf{C}$ is considered by updating it at the initial iteration of every time step, as suggested by [10], in order to avoid convergence issues.

6 EQUIVALENT EARTHQUAKE FORCES

An analytical model is proposed to determine the equivalent earthquake forces $\mathbf{p}(t)$ (equation (9)), which are derived from accelerograms. This model assumes that no movement occurs at the foundation level of a structure submitted to earthquake loads, as the respective degrees of freedom are constrained. The equivalent earthquake forces are applied to the remaining unconstrained degrees of freedom.

The actual behavior of the structure demonstrates that every degree of freedom is in motion while earthquake loads are applied at the foundation level, in response to ongoing ground accelerations. For this actual model, equation (9) is rewritten as

$$\begin{bmatrix} \mathbf{M}_{FF} & \mathbf{0} \\ \mathbf{0} & \mathbf{M}_{RR} \end{bmatrix}\begin{bmatrix} \ddot{\mathbf{u}}_F(t) \\ \ddot{\mathbf{u}}_R(t) \end{bmatrix} + \begin{bmatrix} \mathbf{f}_F(\mathbf{u}(t)) \\ \mathbf{f}_R(\mathbf{u}(t)) \end{bmatrix} = \begin{bmatrix} \mathbf{0} \\ \mathbf{p}_R(t) \end{bmatrix} \tag{15}$$

where subscripts R and F represent the degrees of freedom that are restrained and free to move in the analytical model, respectively. The effects of damping are neglected. Restoring force vector $\mathbf{f} = [\mathbf{f}_F \quad \mathbf{f}_R]^T$ is nonlinearly defined by equation (3). It is assumed that no other forces but earthquake loads at the foundation level are applied, i.e. $\mathbf{p}_F(t) = \mathbf{0}$.

The analytical model is produced by removing the rigid body movement associated with the foundation degrees of freedom from the actual model. Ground acceleration is denoted as $\ddot{\bar{\mathbf{u}}}(t) = \left[\ddot{\bar{\mathbf{u}}}_F(t) \quad \ddot{\bar{\mathbf{u}}}_R(t)\right]^T$, such that $\ddot{\mathbf{u}}_R - \ddot{\bar{\mathbf{u}}}_R = \mathbf{0}$. As stresses and strains are not affected by rigid body movements, the analytical restoring force vector is $\mathbf{f}(\mathbf{u} - \bar{\mathbf{u}}) = \mathbf{f}(\mathbf{u})$. Therefore, the analytical model is defined by

$$\begin{bmatrix} \mathbf{M}_{FF} & \mathbf{0} \\ \mathbf{0} & \mathbf{M}_{RR} \end{bmatrix}\begin{bmatrix} \ddot{\mathbf{u}}_F(t) - \ddot{\bar{\mathbf{u}}}_F(t) \\ \mathbf{0} \end{bmatrix} + \begin{bmatrix} \mathbf{f}_F(\mathbf{u}(t)) \\ \mathbf{f}_R(\mathbf{u}(t)) \end{bmatrix} = \begin{bmatrix} \mathbf{p}_F^*(t) \\ \mathbf{p}_R^*(t) \end{bmatrix} \tag{16}$$

The analytical external forces at the free-to-move degrees of freedom are given by subtracting equation (15) from equation (16), i.e. $\mathbf{p}_F^*(t) = -\mathbf{M}_{FF}\ddot{\bar{\mathbf{u}}}_F(t)$. As $\mathbf{p}_F^*(t)$ is not given in terms of $\mathbf{f}(\mathbf{u})$, this model is suitable for both linear and nonlinear systems. Hence, $\mathbf{p}(t)$ is evaluated as

$$\mathbf{p}(t) = -\mathbf{M}_{FF}\ddot{\bar{\mathbf{u}}}_F(t) \tag{17}$$

7 EXAMPLE: REINFORCED CONCRETE BUILDING IN RIO BRANCO, AC

The presented methodology was implemented in C++ and applied to an example that investigates a RC building submitted to a hypothetical earthquake in Rio Branco, Acre (AC), Brazil. According to [1], this area is designated as Seismic Zone 2. The corresponding characteristic horizontal seismic acceleration is $a_g = 0.10g$, where $g = 9.80665\ \text{m/s}^2$ is the gravitational acceleration, and the soil is classified as class D (stiff soil). For such particulars, artificial earthquake data was generated using the software Artquake v.3.10, developed by [11]. The theoretical and generated response spectra showed great resemblance, satisfying the criteria of [1] to allow for the use of artificial data.

Reference [1] requires that at least three analyses are performed using different sets of accelerograms. Each set is comprised of two accelerograms simultaneously applied to both horizontal directions

(x and y axes). In this study, six accelerograms were generated and randomly paired up in three sets (Fig. 3). Earthquakes are 20 seconds long, and 3000 time steps are integrated.

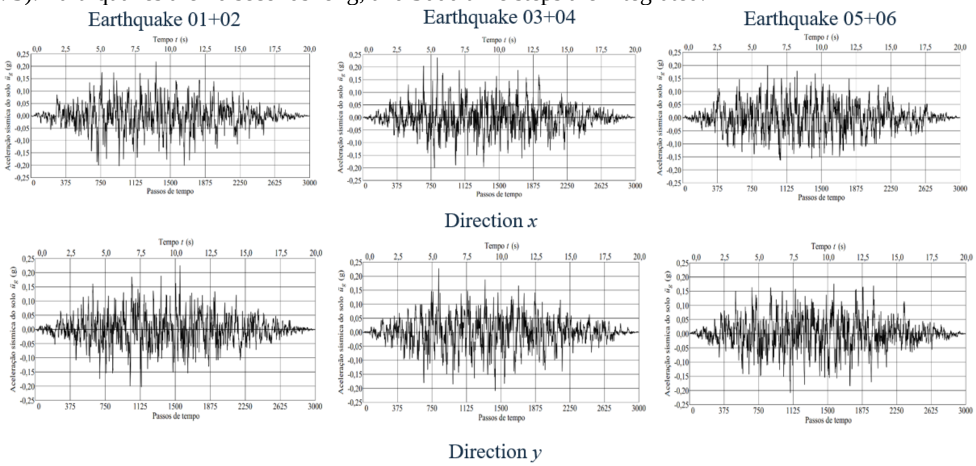

Fig. 3 Sets of artificial accelerograms simulating typical earthquakes in Rio Branco, AC, Brazil.

The structure is a four-story building designed as an outpatient clinic. Fig. 4 shows its physical and geometric properties. In order to apply the frame finite element described in section 2, all cross-sections are considered to be rectangular. Dead and live loads are determined according to [12] and [13]. In each floor, slab loads are uniformly distributed across beam elements through influence areas. It is assumed live loads do not contribute to structural mass.

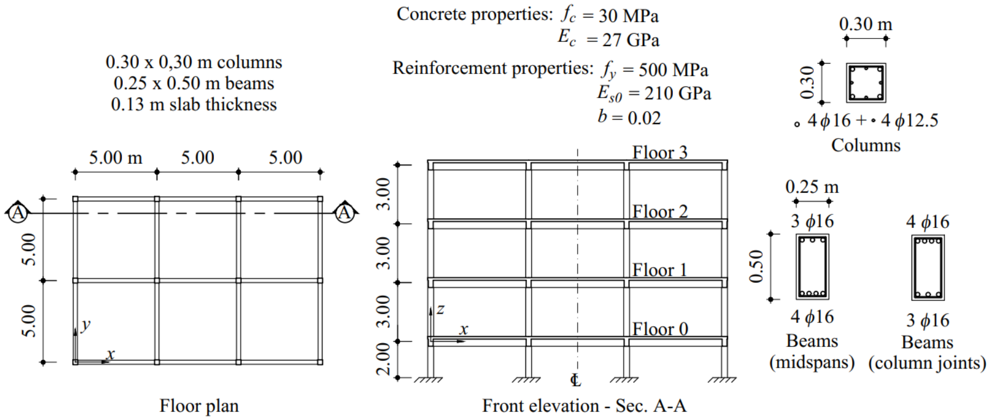

Fig. 4 Physical and geometric properties of four-story building in Rio Branco, AC, Brazil.

All cross-sections are verified at the Ultimate Limit State (ULS) in two load stages: prior to and during the earthquake. At the first stage, partial safety factors for dead loads, live loads, steel and concrete are $\gamma_g = 1.4$, $\gamma_q = 1.4$, $\gamma_s = 1.15$ and $\gamma_c = 1.4$, respectively, per [12]. This initial nonlinear analysis shows that both the maximum steel strain ($\varepsilon_{s,\max} = 0.0015$) and the minimum concrete strain ($\varepsilon_{c,\min} = -0.0006$) meet the ULS criteria stablished by [12], i.e. steel and concrete strains are limited to $\varepsilon_{s,\max} = 0.010$ and $\varepsilon_{c,\min} = -0.0035$, respectively. No convergence issues were reported.

At the earthquake load stage, partial safety factors are $\gamma_c = 1.2$, $\gamma_q = 1.0$, $\gamma_s = 1.0$ and $\gamma_c = 1.2$, as an exceptional load combination should be considered according to [1]. A combination factor $\psi_0 = 0.7$ is applied to live loads, as suggested by [14]. To determine damping matrix $\mathbf{C}$, a study on the primary modal frequencies of the associated undamped system is performed, and the damping ratio is considered as $\zeta = 5\%$. In evaluating equation (10), it is assumed that $c_1 = 0.0577$ and $c_2 = 0.0433$. No convergence issues were reported in any of the three analyses performed at this stage.

Nodal displacements are measured at floor 3 (Fig. 4). The critical displacement in history, in modulus, is $\left(\delta_x^{\ 2} + \delta_y^{\ 2}\right)^{1/2} = 0.050\ \text{m}$, obtained from the analysis of the set of accelerograms Earthquake 01+02 (Fig. 3), where δ_x and δ_y are the nodal displacements in directions *x* and *y*, respectively. This displacement is considered to be consistent with this example's input data.

Reference [1] demands displacement response to be given by a displacement-time envelope curve, considering all sets of accelerograms in analysis. The envelope curves for the critical nodal displacements in directions *x* and *y* are shown in Fig. 5. The maximum and minimum values from the envelope curves should be multiplied by factor C_d / R_m , where $C_d = 2.5$ and $R_m = 3$ for RC frame structures. Therefore, the analytical maximum and minimum nodal displacements are $\delta_{x,máx} = 0.037\ \text{m}$ and $\delta_{x,mín} = -0.032\ \text{m}$, in the *x* direction, and $\delta_{y,máx} = 0.033\ \text{m}$ and $\delta_{y,mín} = -0.035\ \text{m}$, in the *y* direction.

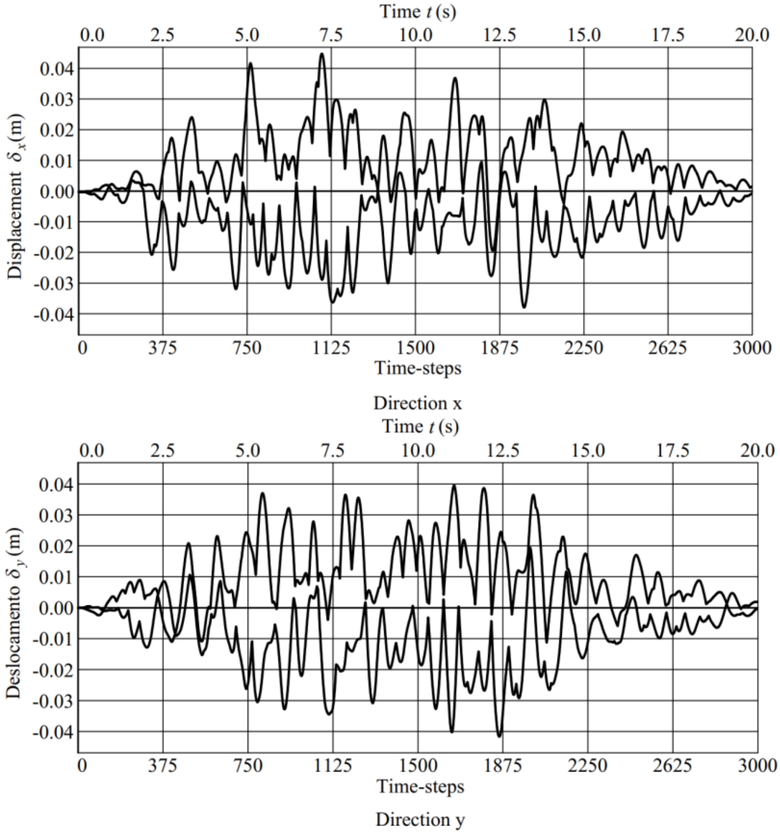

Fig. 5 Displacement-time envelope curves in the *x* and *y* directions.

8 CONCLUSIONS

The time-domain approach in dynamic analysis proves suitable for design purposes and adheres to the guidelines outlined in [1], providing a rigorous methodology for the nonlinear analysis of structures in regions susceptible to seismic activity and critical facilities in Brazil. The application example demonstrates the capabilities of the methodology, implemented as a computational tool developed in C++. The example presents a RC building in Rio Branco, Acre, submitted to earthquake loads. Three analyses were performed using artificial accelerograms and following Brazilian standards [1], [12], [13] and [14]. The maximum displacement in modulus (0,050 m) aligns with expected results for this case, demonstrating the reliability of the approach. The critical nodal displacements from the three sets of accelerograms analyzed, as shown in the displacement-time envelope curve (Fig. 5), multiplied by factor C_d / R_m, range from $\delta_{x,máx} = 0.037$ m to $\delta_{x,mín} = -0.032$ m, in the *x* direction, and from $\delta_{y,máx} = 0.033$ m to $\delta_{y,mín} = -0.035$ m, in the *y* direction. The effectiveness of the methodology is demonstrated by the analyses completing successfully without any convergence issues.

Acknowledgements

The authors gratefully acknowledge Prof. Sergio Hampshire de Carvalho Santos and Prof. Silvio de Souza Lima from the Universidade Federal do Rio de Janeiro for their valuable suggestions, contributions to this research, and access to the ArtQuake program. The first author also thanks CAPES (Coordenação de Aperfeiçoamento de Pessoal de Nível Superior) for financial support.

References

[1] Brazilian Association of Technical Standards. 2023. "*ABNT NBR 15421: Design of seismic resistant structures*." Rio de Janeiro, Brazil.

[2] Braz, Luiz Fernando C. R. and Schulz, Mauro. 2021. "Estabilidade de estruturas tubulares em situação de içamento." *Revista da Estrutura de Aço - REA*, vol. 10, n. 3:312–332.

[3] Cowper, G. R. 1966. "The shear coefficient in Timoshenko's beam theory." *Journal of Applied Mechanics*, v. 33:335–340.

[4] Kent, D. C. and Park, R. 1971. "Flexural members with confined concrete." *Journal of the Structural Division*, ASCE, 97(ST7).

[5] Scott, B. D., Park, R. and Priestley, M. J. N. 1982. "Stress-strain behavior of concrete confined by overlapping hoops at low and high strain rates." *ACI Journal*, v. 79, n. 1:13–27.

[6] Karsan, L. D. and Jirsa, J. O. 1969. "Behavior of concrete under compressive loadings." *Journal of the Structural Division*, ASCE, 95(ST12).

[7] M. Menegotto and P. E. Pinto. 1973. "Method of analysis for cyclically loaded R.C. plane frames including changes in geometry and non-elastic behaviour of elements under combined normal force and bending." In Preliminary Report 13:15–22, IABSE Symp. on Resistance and Ultimate Deformability of Structures Acted on by Well Defined Repeated Loads, Lisbon.

[8] Filippou, F. C., Popov. E P. and Bertero, V. V. 1983. "Effects of bond deterioration on hysteretic behavior of reinforced concrete joints." *Report No. UCB/EERC–83/19*, Earthquake Engineering Research Center, University of California, Berkeley.

[9] Chopra, A. K. 2012. "Dynamics of structures: Theory and applications to earthquake engineering." 4th ed., Upper Saddle River, NJ, United States: Pearson Education.

[10] Filippou, F. C., D'Ambrisi, A. and Issa, A. 1992. "Nonlinear Static and Dynamic Analysis of Reinforced Concrete Subassemblages." *Report No. UCB/EERC–92/08*, Earthquake Engineering Research Center, University of California, Berkeley.

[11] Rodrigues, Rodrigo M. R., Santos, Sérgio H. C. and Lima, Sílvio S. 2012. *"Geração de acelerogramas sísmicos artificiais compatíveis com um espectro de resposta."* B.S. thesis, Escola Politécnica, UFRJ, Rio de Janeiro, RJ.

[12] Brazilian Association of Technical Standards. 2023. "*ABNT NBR 6118: Design of concrete structures – Procedure*." Rio de Janeiro, Brazil.

[13] Brazilian Association of Technical Standards. 2019. "*ABNT NBR 6120: Design of concrete structures – Procedure*." Rio de Janeiro, Brazil.

[14] Brazilian Association of Technical Standards. 2004. "*ABNT NBR 8681: Actions and safety of concrete structures – Procedure*." Rio de Janeiro, Brazil.